

## TIPP 2011 - Technology and Instrumentation for Particle Physics 2011

### An Apparatus to Search for Neutrinoless Double Beta Decay

R. B. Pahlka (for the NEMO-3 and SuperNEMO Collaborations)<sup>1</sup>

*Fermi National Accelerator Laboratory, P. O. Box 500, Batavia, IL 60510, USA*

#### Abstract

The NEMO-3 (Neutrino Ettore Majorana Observatory) experiment, located in the Modane Underground Laboratory, searches for neutrinoless double beta decay. The experiment has been taking data since 2003 with seven double beta isotopes and completed data acquisition in January 2011. Two neutrino double beta decay results for the main isotopes (7 kg of <sup>100</sup>Mo and 1 kg of <sup>82</sup>Se), new results for <sup>150</sup>Nd and <sup>130</sup>Te, as well as results for <sup>96</sup>Zr and <sup>48</sup>Ca are presented. NEMO-3 uses a unique technique that allows for the *in situ* measurement of background contamination. No evidence for neutrinoless double beta decay has been found to date. The data are also interpreted in terms of alternative models such as weak right-handed currents and Majoron emission. In this proceeding, I discussed the measurements made with NEMO-3 and discussed the status, research and design of the next generation experiment, SuperNEMO.

© 2012 Published by Elsevier B.V. Selection and/or peer review under responsibility of the organizing committee for TIPP 11. Open access under [CC BY-NC-ND license](#).

**Keywords:** NEMO-3, SuperNEMO, neutrinoless double beta decay

#### 1. Introduction

The observation of neutrino oscillations and the resulting measurements of the neutrino mass squared differences has motivated measurements of the absolute neutrino mass. Neutrinoless double beta decay ( $0\nu\beta\beta$ ) is one of the only practical ways to understand the nature of neutrino mass and one of the most sensitive probes of its absolute value. Proposed by Ettore Majorana, neutrinos could be their own anti-particles [1], which led to Furry's conclusion [2] that neutrinoless double beta decay is possible via neutrino exchange if the neutrinos are Majorana particles and have non-zero mass.

Double beta decay is a rare nuclear process in which two neutrons in the same nucleus are spontaneously converted into two protons. This process occurs when single beta decay is either forbidden or suppressed, and may happen in at least two different ways: by the emission of two electrons and two anti-electron neutrinos (already observed in many nuclei), or possibly by the emission of two electrons, but no neutrinos. The effective Majorana neutrino mass  $\langle m_{\beta\beta} \rangle$  is proportional to the square root of the  $0\nu\beta\beta$  decay half-life  $T_{1/2}^{0\nu}$ , where  $G^{0\nu}$  is the kinematic phase-space factor and  $M_{0\nu}$  is the nuclear matrix element and is given as

$$[T_{1/2}^{0\nu}]^{-1} = G^{0\nu} |M_{0\nu}|^2 \langle m_{\beta\beta} \rangle^2. \quad (1)$$

<sup>1</sup>pahlka@fnal.gov

The experimental signature of  $0\nu\beta\beta$  is two electrons with the energy sum equaling the  $Q_{\beta\beta}$  of the decay. There are other mechanisms to explain neutrinoless double beta decay [3], but the above mechanism is the most favored due to the minimal required modifications to the Standard Model. There are several consequences if the neutrino is found to be a Majorana particle. It would imply lepton conservation violation which is required by some GUT theories. It would also give access to CP violation phases, which cannot be easily measured by neutrino oscillation experiments. Finally, it would provide a natural explanation of the small mass of the neutrino and it could help explain the matter/anti-matter asymmetry in the Universe through leptogenesis.

## 2. The NEMO-3 Detector

The goal of the NEMO-3 experiment is to search for  $0\nu\beta\beta$  decay with a half-life sensitivity of  $10^{24}$  -  $10^{25}$  years, which can probe the effective Majorana neutrino mass  $\langle m_\nu \rangle$  down to the level of 0.1-0.3 eV. The NEMO-3 detector employs a tracking chamber and a calorimeter to measure  $2\nu\beta\beta$  decay and search for  $0\nu\beta\beta$  decay in several isotopes. The detector is installed in the Laboratoire Souterrain de Modane located in the Fréjus tunnel in Modane, France. It is azimuthally divided into twenty identical wedge sectors each assembled as a tracking chamber and calorimeter [4] enclosing a vertically-fixed double beta isotopic foil. This technique allows the study of several double beta decay observables including the individual electron energies, their associated angular distributions, the event vertex within the source, and the particle flight time. This heterogeneous method where the source and the detector are separated allows for precision measurements of backgrounds. The segmented calorimeter provides good energy measurements with an energy resolution of  $\sim 14\%$  (FWHM) at 1 MeV and good timing resolution of  $\sim 250$  ps. With a cylindrical detector design, the tracking chamber provides good spatial resolution of the foil and scintillator vertices with  $\sim 0.6$  cm  $\sigma$  in the  $(R\phi)$  direction and  $\sim 1.0$  cm  $\sigma$  in the Z-direction. The NEMO-3 detector identifies electrons, positrons, gammas, and  $\alpha$ -particles originating from multi-particle events in the low energy domain of natural radioactivity. The source foils are fixed vertically in the detector and are either metallic or composite. There are seven double beta decay sources, a copper foil, and a natural tellurium foil. Figure 1 shows a rendering of the detector including the source foils, tracking chamber, and calorimeter modules. It also shows the breakdown of the isotopic foils installed in the detector.

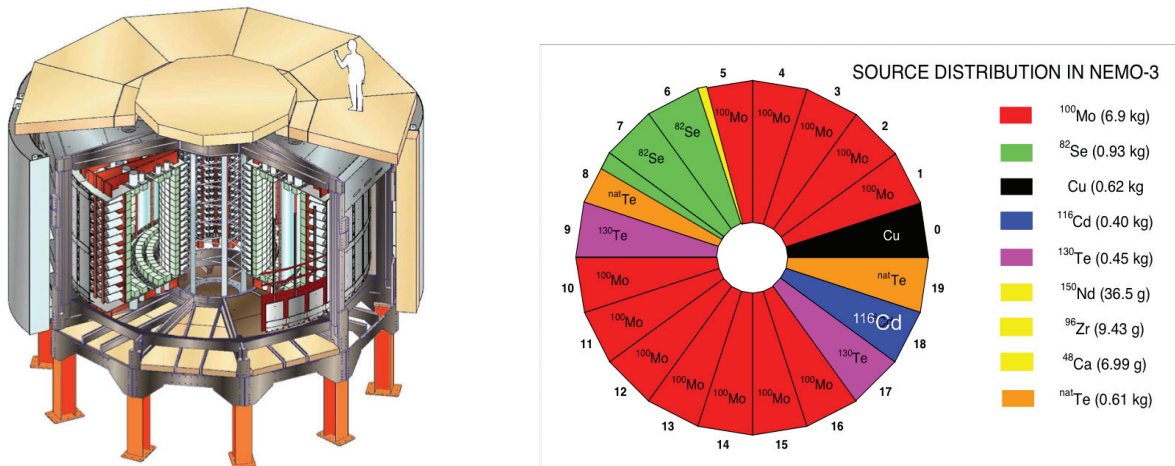


Figure 1: Left-hand side: A rendering of the NEMO-3 detector. Right-hand side: The configuration and arrangement of the seven double beta isotopic sources installed in the detector.

## 3. BACKGROUNDS IN NEMO-3

For the various mechanisms of neutrinoless double beta decay, the backgrounds come from two main sources. The first is the irreducible background from the tail of the  $2\nu\beta\beta$  decay distribution which inherently cannot be separated

from the  $0\nu\beta\beta$  signal due to the finite energy resolution of the detector. The second is background events due to contamination originating from the  $^{238}\text{U}$ ,  $^{235}\text{U}$  and  $^{232}\text{Th}$  decay chains including the large Q-value isotopes of  $^{214}\text{Bi}$  and  $^{208}\text{Tl}$ .

A description of all external and internal backgrounds has been reported previously [5]. A unique advantage of NEMO-3 is the capability to identify and measure the detector backgrounds *in situ* with high precision. To decrease the external cosmic ray background for the NEMO-3 detector, it was placed at a depth of 4800 meters of water equivalent (MWE) where the cosmic ray flux has been found to be negligible. Iron and water shielding as well as a magnetic field suppress the backgrounds from  $\gamma$ -rays and neutrons. The robust air ventilation system in the laboratory combined with the radon tent surrounding the detector reduces radon levels down to  $6 \text{ Bq/m}^3$ . The internal background for the source foils comes from contamination from natural sources originating during the production of the foil. These include the daughter nuclei of  $^{234m}\text{Pa}$  and  $^{228}\text{Ac}$  which give rise to  $^{222}\text{Rn}$  and  $^{220}\text{Rn}$ , with subsequent generation of the pernicious isotopes  $^{214}\text{Bi}$  and  $^{208}\text{Tl}$ . There is also contamination from various amounts of  $^{40}\text{K}$ ,  $^{90}\text{Sr}$ ,  $^{137}\text{Cs}$ , and isotopes associated with the  $^{235}\text{U}$  decay chain.

The NEMO-3 detector is capable of distinguishing between internal and external events based on the time at which at least two scintillators are fired. We consider two hypotheses. In the *internal* hypothesis, we assume that particles originate in the foil, traverse the tracking chamber and are registered in the calorimeter. In the *external* hypothesis, we assume that particles originate in the detector (outside the foil), interact with the foil and register two or more calorimeter hits. In each hypothesis, we calculate the time difference between each of the particles and compare this to the measured time difference from the calorimeter.

#### 4. Results

Table 1 shows the  $Q_{\beta\beta}$  value, the isotopic abundance, results of measurements of the  $2\nu\beta\beta$  half-lives, and lower limits on the  $0\nu\beta\beta$  half-lives for the isotopes installed in the detector.

Isotope	$Q_{\beta\beta}$ (keV)	Abundance (%)	$T_{1/2}^{2\nu\beta\beta}$ (y)	$T_{1/2}^{0\nu\beta\beta} >$ (y)
$^{130}\text{Te}$	2529	33.8	$(7.0 \pm 0.9(\text{stat}) \pm 1.1(\text{syst})) \times 10^{20}$	$1.3 \times 10^{23}$ [7]
$^{116}\text{Cd}$	2805	7.5	$(2.88 \pm 0.04(\text{stat}) \pm 0.16(\text{syst})) \times 10^{19}$	$1.3 \times 10^{23}$
$^{82}\text{Se}$	2995	9.2	$(9.6 \pm 0.1(\text{stat}) \pm 1.0(\text{syst})) \times 10^{19}$	$3.2 \times 10^{23}$
$^{100}\text{Mo}$	3035	9.6	$(7.17 \pm 0.01(\text{stat}) \pm 0.54(\text{syst})) \times 10^{18}$	$1.0 \times 10^{24}$
$^{96}\text{Zr}$	3350	2.8	$(2.35 \pm 0.14(\text{stat}) \pm 0.16(\text{syst})) \times 10^{19}$	$9.2 \times 10^{21}$ [8]
$^{150}\text{Nd}$	3367	5.6	$(9.11^{+0.25}_{-0.22}(\text{stat}) \pm 0.63(\text{syst})) \times 10^{18}$	$1.8 \times 10^{22}$ [9]
$^{48}\text{Ca}$	4272	0.187	$(4.4^{+0.5}_{-0.4}(\text{stat}) \pm 0.4(\text{syst})) \times 10^{19}$	$1.3 \times 10^{22}$

Table 1: The  $Q_{\beta\beta}$  value, the isotopic abundance, results of measurements of the  $2\nu\beta\beta$  half-lives, and lower limits on the  $0\nu\beta\beta$  half-lives for the isotopes installed in the NEMO-3 detector.

Using a likelihood ratio, we observe no events above background and thus exclude additional contributions via the light Majorana neutrino exchange mechanism at a level which corresponds to a lower limit on the  $0\nu\beta\beta$  half-life of  $T_{1/2}^{0\nu\beta\beta} > 1.0 \times 10^{24}$  (90% CL) for  $^{100}\text{Mo}$  and  $T_{1/2}^{0\nu\beta\beta} > 3.2 \times 10^{23}$  (90% CL) for  $^{82}\text{Se}$ . Figure 2 shows the two electron energy sum distributions for the  $^{100}\text{Mo}$  source and the  $^{82}\text{Se}$  source data, the sum of the backgrounds, the  $2\nu\beta\beta$  spectrum and the  $0\nu\beta\beta$  limit for the expected neutrinoless double beta decay events. The lower limit on the half-life is translated into an upper limit on the effective Majorana neutrino mass,  $\langle m_\nu \rangle$  such that  $\langle m_\nu \rangle < 0.47 - 0.96 \text{ eV}$  and  $\langle m_\nu \rangle < 0.9 - 2.5 \text{ eV}$  for  $^{100}\text{Mo}$  and  $^{82}\text{Se}$ , respectively.

Using the NEMO-3 detector, we also investigate alternative models that predict emission of Goldstone bosons (Majorons) that couple to the neutrino as well as neutrino coupling through right-handed currents (V+A). Additionally, due to the calorimeter segmentation and track identification, we are able to measure  $2\nu\beta\beta$ - and probe  $0\nu\beta\beta$ -decay to excited states.

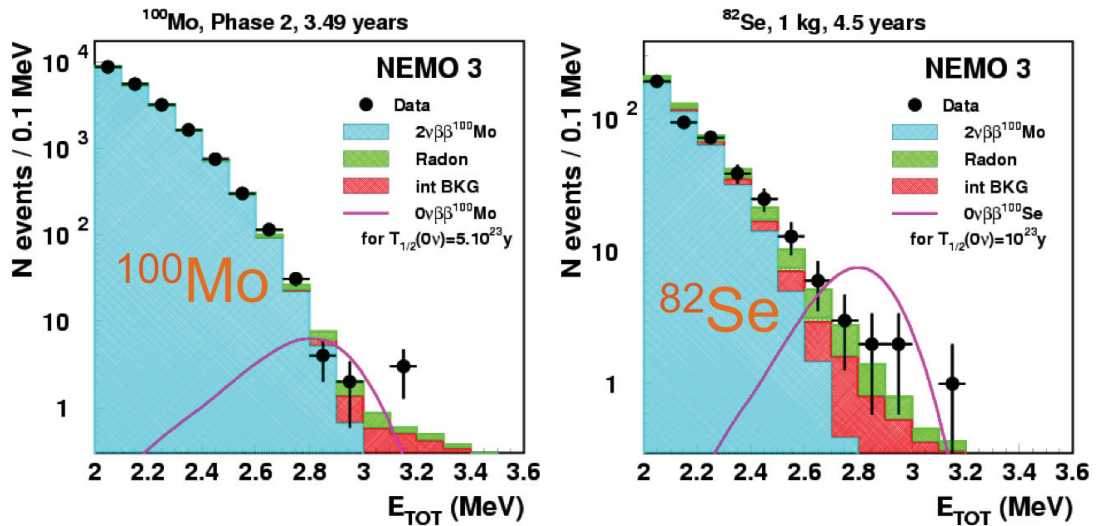


Figure 2: Left-hand side: The electron energy sum distribution for  $^{100}\text{Mo}$ . Right-hand side: The electron energy sum distribution for  $^{82}\text{Se}$ . Data are shown as black dots along with the internal and external background distributions and the expected neutrinoless double beta decay signal.

## 5. Dismantling of NEMO-3

The dismantling of the NEMO-3 detector has been completed. Figure 3 shows some of the progress in dismantling. The Collaboration has reclaimed the source foils, scintillator blocks, and many of the PMTs installed in the detector. Careful consideration of source foil contamination was taken.

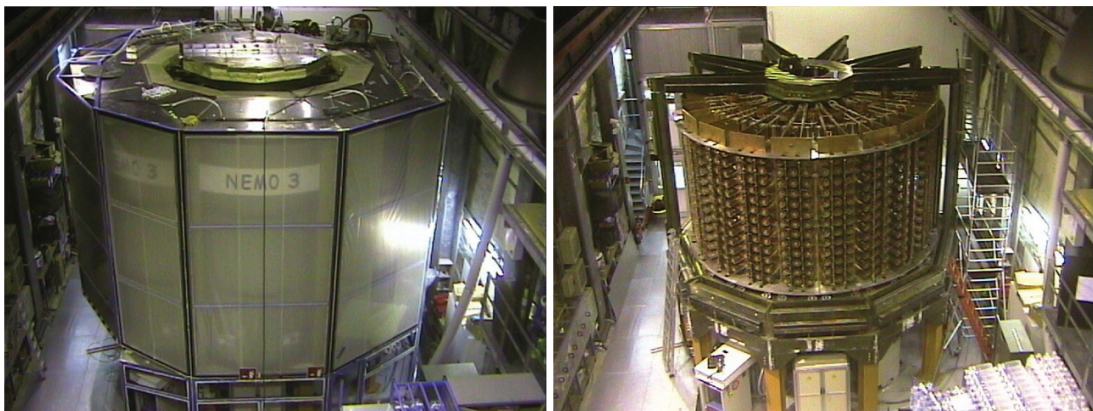


Figure 3: Left-hand side: Before dismantling, showing the full detector with some top access panels removed. Right-hand side: During dismantling, showing the removal of the radon tent, and the iron and water shields.

## 6. The SuperNEMO Detector

SuperNEMO is a  $\sim 100$  kg source isotope ( $^{82}\text{Se}$  or  $^{150}\text{Nd}$ ), tracker + calorimeter detector with a target neutrinoless double beta decay half-life sensitivity of  $10^{26}$  years ( $\sim 50$  meV effective Majorana neutrino mass). To fulfill these physics goals, SuperNEMO will build upon the NEMO-3 technology choice of combining calorimetry and tracking. This gives the ability to measure individual electron tracks, vertices, energies and time of flight, and to reconstruct fully



the kinematics and topology of an event. Particle identification of gamma and alpha particles, as well as distinguishing electrons from positrons with the help of a magnetic field, form the basis of background rejection. An important feature of NEMO-3 which is kept in SuperNEMO is the fact that the double beta decay source is separate from the detector, allowing several different isotopes to be studied. SuperNEMO will consist of about twenty identical modules, each housing around 5–7 kg of isotope. The project is completing a 3 year design study and R&D phase with much progress towards the first prototype demonstrator module. The Collaboration comprises over 90 physicists from 12 countries. The R&D program focuses on four main areas of study: isotope enrichment, tracking detector, calorimeter, and ultra-low background materials production and measurements. The expected improvement in performance of SuperNEMO compared to its predecessor NEMO-3 is shown in Table 2 which compares the parameters of the two experiments. The most important design study tasks are described in the sections that follow.

	NEMO 3	SuperNEMO
isotope	$^{100}\text{Mo}$	$^{150}\text{Nd}$ or $^{82}\text{Se}$
mass	7 kg	100–200 kg
signal efficiency	8%	> 30%
$^{208}\text{Tl}$ in foil	< $20\mu\text{Bq/kg}$	< $2\mu\text{Bq/kg}$
$^{214}\text{Bi}$ in foil	< $300\mu\text{Bq/kg}$	< $10\mu\text{Bq/kg}$ ( $^{82}\text{Se}$ )
energy resolution at 3 MeV	8% (FWHM)	4% (FWHM)
half-life	$T_{1/2}^{0\nu} > 2 \cdot 10^{24}$ years	$T_{1/2}^{0\nu} > 1 - 2 \cdot 10^{26}$ years
neutrino mass	$\langle m_{\beta\beta} \rangle < 0.2 - 0.5$ eV	$\langle m_{\beta\beta} \rangle < 50 - 90$ meV

Table 2: Comparison of the main NEMO-3 and SuperNEMO parameters.

Figure 4 shows two renderings of the SuperNEMO demonstrator module. The source is a thin ( $\sim 40$  mg/cm) foil inside the detector. It is surrounded by a gas tracking chamber followed by calorimeter walls. The tracking volume contains more than 2000 wire drift chambers operated in Geiger mode, which are arranged in nine layers parallel to the foil. The calorimeter is divided into  $\sim 1000$  blocks which cover most of the detector outer area and are read out by photo multiplier tubes (PMT).

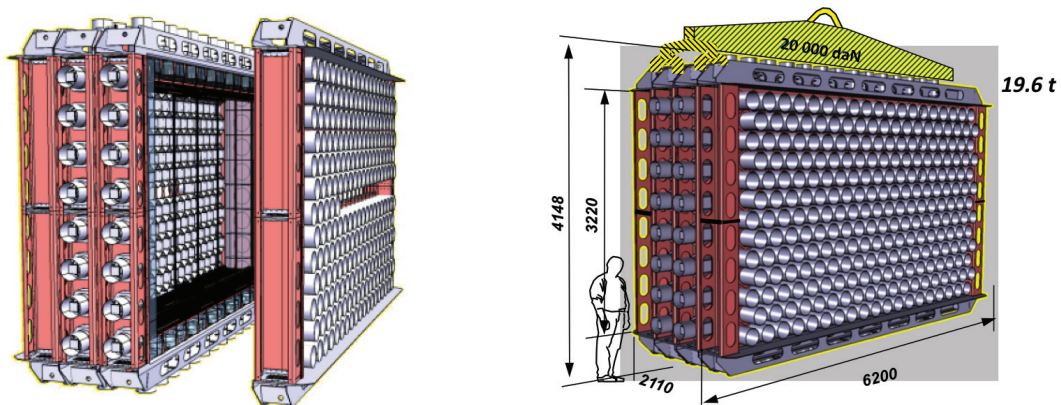


Figure 4: Preliminary design of the SuperNEMO detector. Left-hand side: An exploded view showing the tracking chamber and calorimeter modules. Right-hand side: A view showing the hexagonal configuration of the calorimeter modules with dimensions.

### 6.1. Calorimeter R&D

SuperNEMO aims to improve the calorimeter energy resolution to  $7\%/\sqrt{E}$  at FWHM (4 % @ the  $Q_{\beta\beta}$  energy). To reach this goal, several studies have been completed on the choice of calorimeter parameters such as scintillator

material (organic plastic or liquid), and the shape, size and coating of calorimeter blocks. These are combined with dedicated development of PMTs with low radioactivity and high quantum efficiency.

The SuperNEMO baseline design calls for large scintillator blocks (  $25 \times 25$  cm). Scintillators of this size read out through a lightguide showed an energy resolution of 9–10% at 1 MeV. Better results have been achieved by casting a large plastic hexagonal shaped scintillator directly on a hemispherical 8" PMT. With this configuration we have been able to reach the important milestone of 7–8% (FWHM) energy resolution for the baseline detector design. Consequently the R&D on solid scintillators will be focusing on cast scintillator solutions rather than lightguides to increase the light collection efficiency. The development program has focused on hexagonal scintillator geometries and long scintillator bars, with the former as the design decision.

Using the latest achievements in PMT, reflector, and scintillator technology the SuperNEMO Collaboration has demonstrated the feasibility of achieving the target energy resolution necessary to reach the sensitivity goal of the experiment. The remaining challenge is to demonstrate that the achieved energy resolution can be maintained at the mass production scale. The large scale construction will start in 2012 with the aim to reach the target sensitivity of  $\langle m_{\beta\beta} \rangle = 50\text{--}100$  meV by 2017. Figure 5 shows a photo of a prototype PVT-based plastic scintillator to be used in SuperNEMO.

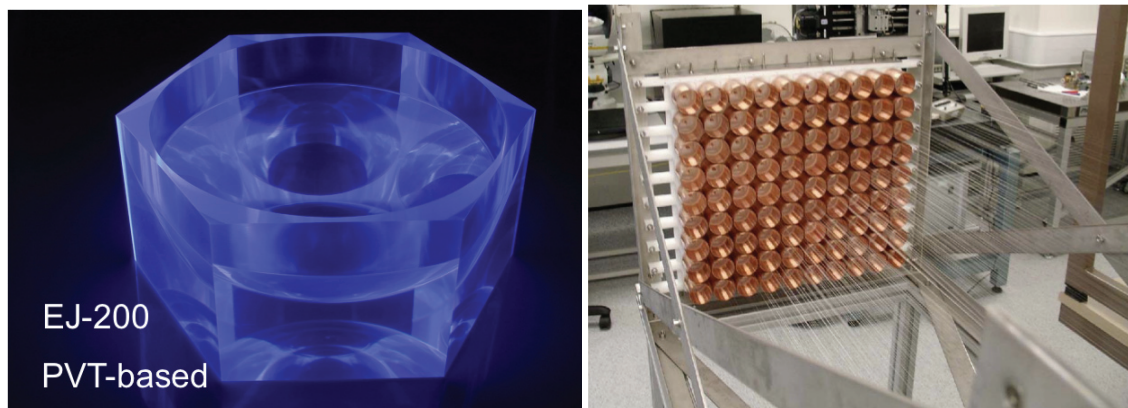


Figure 5: Left-hand side: A photo of a prototype scintillator to be used in SuperNEMO. Right-hand side: A 90-cell tracking chamber prototype.

## 6.2. Tracker design

The SuperNEMO tracker consists of octagonal wire drift cells operated in Geiger mode. Each cell is around 4 m long and has a central anode wire surrounded by 8–12 ground wires, with cathode pickup rings at both ends. Signals can be read out from the anode and/or cathodes to determine the position at which the ionising particle crossed the cell.

The tracking detector design study looks at optimising its parameters to obtain high efficiency and resolution in measuring the trajectories of double beta decay electrons, as well as of alpha particles for the purpose of background rejection. The tracking chamber geometry is being investigated with the help of detector simulations to compare the different possible layouts. In addition, several small prototypes have been built to study the drift chamber cell design and size, wire length, diameter and material, and gas mixture [11].

The first 9-cell prototype was successfully operated with three different wire layouts, demonstrating a plasma propagation efficiency close to 100% over a wide range of voltages [11]. In addition, a 90-cell prototype has recently been constructed which will test the mechanics and large-scale operation of the drift cell system. A SuperNEMO module will contain several thousand drift cells with 8–12 wires each. The large total number of wires requires an automated wiring procedure, thus a dedicated wiring robot is being developed for the mass production of drift cells.

## 6.3. Choice of source isotope

The choice of isotope for SuperNEMO is aimed at maximizing the neutrinoless signal over the background of two-neutrino double beta decay and other background events. Therefore the isotope must have a long two-neutrino

half-life, and high endpoint energy and phase space factor  $G_{0\nu} (T_{1/2}^{0\nu} \sim G_{0\nu}^{-1})$ . The enrichment possibility on a large scale is also a factor in selecting the isotope. The main candidate isotopes for SuperNEMO have emerged to be  $^{82}\text{Se}$  and  $^{150}\text{Nd}$ . A sample of 5 kg of  $^{82}\text{Se}$  has been enriched and is currently undergoing purification. The SuperNEMO Collaboration has also investigated the possibility of enriching large amounts of  $^{150}\text{Nd}$  via the method of atomic vapor laser isotope separation.

#### 6.4. Radiopurity of the source

SuperNEMO will search for a very rare process, therefore it must maintain ultra-low background levels. The source foils must be radiopure, and their contamination with naturally radioactive elements must be precisely measured. The most important source contaminants are  $^{208}\text{Tl}$  and  $^{214}\text{Bi}$ , whose decay energies are close to the neutrinoless double beta decay signal region. SuperNEMO requires source foil contamination to be less than  $2\mu\text{Bq/kg}$  for  $^{208}\text{Tl}$  and less than  $10\mu\text{Bq/kg}$  for  $^{214}\text{Bi}$ .

In order to evaluate these activities, a dedicated “BiPo” detector was developed which can measure the signature of an electron followed by a delayed alpha particle. The first BiPo prototype (BiPo1) was installed in the Modane Underground Laboratory in February 2008 and is currently running with 20 modules. The objective for this prototype is to measure the backgrounds and surface contamination of the prototype’s plastic scintillators. After three months, an upper limit on the sensitivity for a standard  $12\text{m}^2$  BiPo detector was calculated to be less than  $7.5\mu\text{Bq/kg}$  for  $^{208}\text{Tl}$  (90% C. L.) [12].

A second BiPo prototype (BiPo2) is also in final stages of characterization. This prototype uses large, thin (75 cm x 75 cm x 1 cm) sheets of Bicron plastic scintillator whereby a source foil can be inserted between two sheets. The signal is read out on the sides with arrays of PMTs coupled to custom light guides. The BiPo2 prototype was installed in the Modane Underground Laboratory in July 2008. Measurements are currently underway for surface and bulk scintillator contamination and optical cross-talk.

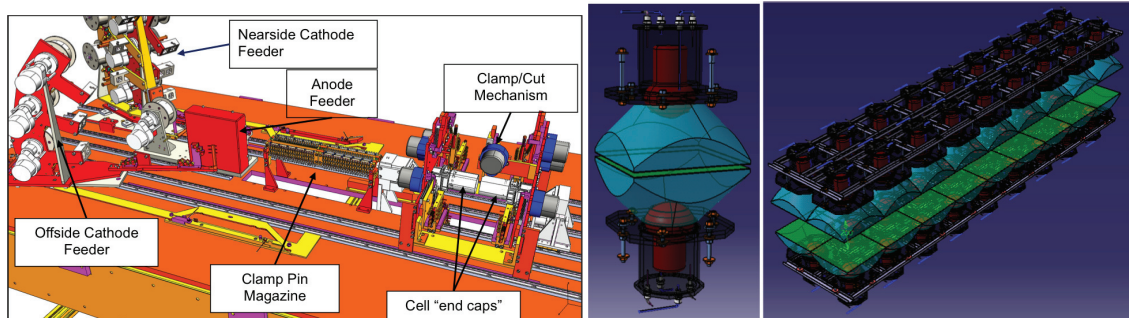


Figure 6: Left-hand side: A schematic of the wiring robot used to string wires for the tracking chamber. Right-hand side: A rendering of the BiPo1 detector.

## 7. Conclusion

The NEMO-3 experiment has been taking data since 2003 with seven double beta isotopes and completed data acquisition in January 2011. Two neutrino double beta decay results for the main isotopes (7 kg of  $^{100}\text{Mo}$  and 1 kg of  $^{82}\text{Se}$ ), new results for  $^{150}\text{Nd}$  and  $^{130}\text{Te}$ , as well as results for  $^{96}\text{Zr}$  and  $^{48}\text{Ca}$  are some of the World’s best. In all isotopes with the data studied so far, we observe no events above background in the neutrinoless double beta decay signal region and place lower limits on these half-lives. This motivates construction of the next generation experiment, SuperNEMO. An extensive R&D program is underway and nearly complete. SuperNEMO will extrapolate the successful technique of calorimetry plus tracking of NEMO-3 to 100 kg of source isotope, aiming to reach a neutrino mass sensitivity of 50 meV. Due to its modular approach, SuperNEMO can start operation in stages, with the first module installed as early as 2012.

[1] E. Majorana, “Theory of the Symmetry of Electrons and Positrons”, Nuovo Cim., 14:171-184, 1937.

- [2] W. Furry, “On Transition Probabilities in Double Beta Disintegration”, *Phys. Rev.*, 56:1184-1193, 1939.
- [3] F. Avignone and others, “Double Beta Decay, Majorana Neutrinos, and Neutrino Mass”, arXiv, nucl-ex:0708.1033, 2007.
- [4] R. Arnold et al., “Technical design and performance of the NEMO 3 detector”, *Nucl. Instrum. Meth.*, A536:79–122, 2005.
- [5] J. Argyriades et al. [ NEMO Collaboration ], “Measurement of the background in the NEMO 3 double beta decay experiment,” *Nucl. Instrum. Meth.* **A606**, 449-465 (2009). [arXiv:0903.2277 [nucl-ex]].
- [6] R. Mohapatra and others, “Theory of Neutrinos: A White Paper”, *Reports on Progress in Physics*, 70:1757-1867, 2007.
- [7] R. Arnold et al. [ NEMO-3 Collaboration ], “Measurement of the Double Beta Decay Half-life of  $^{130}\text{Te}$  with the NEMO-3 Detector,” *Phys. Rev. Lett.* **107**, 062504 (2011). [arXiv:1104.3716 [nucl-ex]].
- [8] J. Argyriades et al. [ NEMO-3 Collaboration ], “Measurement of the two neutrino double beta decay half-life of Zr-96 with the NEMO-3 detector,” *Nucl. Phys.* **A847**, 168-179 (2010). [arXiv:0906.2694 [nucl-ex]].
- [9] J. Argyriades et al. [ NEMO Collaboration ], “Measurement of the Double Beta Decay Half-life of Nd-150 and Search for Neutrinoless Decay Modes with the NEMO-3 Detector,” *Phys. Rev.* **C80**, 032501 (2009). [arXiv:0810.0248 [hep-ex]].
- [10] M. Kauer, “Calorimeter R&D for the SuperNEMO Double Beta Decay Experiment”, arXiv, hep-ex:0807.2188, 2008.
- [11] I. Nasteva, “The SuperNEMO double beta decay experiment ”, arXiv, hep-ex:0710.4279, 2007.
- [12] M. Bongrand, “BiPo Prototype for SuperNEMO Radiopurity Measurements”, *J. Inst.* 3:P06006, 2008.